

## Characterization and the optical switching phenomenon of porous silica dispersed with silver nano-particles within its pores

This article has been downloaded from IOPscience. Please scroll down to see the full text article.

1996 J. Phys.: Condens. Matter 8 L591

(<http://iopscience.iop.org/0953-8984/8/40/004>)

View [the table of contents for this issue](#), or go to the [journal homepage](#) for more

Download details:

IP Address: 171.66.16.207

The article was downloaded on 14/05/2010 at 04:15

Please note that [terms and conditions apply](#).

LETTER TO THE EDITOR

## Characterization and the optical switching phenomenon of porous silica dispersed with silver nano-particles within its pores

Cai Weiping and Zhang Lide

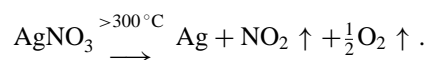
Institute of Solid State Physics, Academia Sinica, Hefei, Anhui 230031, People's Republic of China

Received 11 June 1996

**Abstract.** Porous silica dispersed with silver nano-particles (about 3 nm) within its pores (cages) has been prepared by a new method. The microstructures, particle size distribution and optical absorption have been examined. We have found that in the process of alternating exposure to the ambient air and annealing, this new material assumes a optical switching and memory effect in the visible wave band or a reversible transition between transparency and opacity.

Porous solids with mesoscopic pores and high specific surface area, dispersed with nano-sized particles within their pores, display many unique properties and have received considerable attention in recent years [1–5]. For example, the dispersion of semiconductor ultrafine particles in the pores of porous glass assumes optical switching and optical nonlinearity [5]; polyaniline filaments within a mesoporous channel host (aluminosilicate) have significant conductivity, and this demonstration of a conjugated polymer with mobile charge carriers in nanometer channels represents a step toward the design of nanometer electronic devices [4]. These new materials, however, are significantly different from the recently extensively reported glass–metal colloid composites (films), organic–inorganic nanocomposites (films) or other nanocomposite films [6–9]. Because all the pores in the porous solids are open to the ambience and/or interconnected, the nano-sized phase located within the pores is also in contact with the ambient air. The nano-scaled phase within the pores is small in size and chemically active [10]. Therefore, there inevitably exist interactions between the ambience and the nano-scaled phase, especially metal particles. This has been confirmed by our recent work. We have synthesized a new material by putting silver nano-particles into the mesoscopic pores of porous silica with the help of a new method. This material displays silver nano-particles that are disconnected and highly uniformly dispersed within the pores of the porous silica, and indicates the optical switching phenomenon and memory effect in different ambient conditions. To our knowledge, a metal nano-particle containing porous solid with optical switching and memory effect has not previously been reported. The details are reported in this letter.

Here we present a new method instead of the wet chemical method [11], ion exchange method or colloidal diffusion method. Our synthesis method is based on the following reaction:



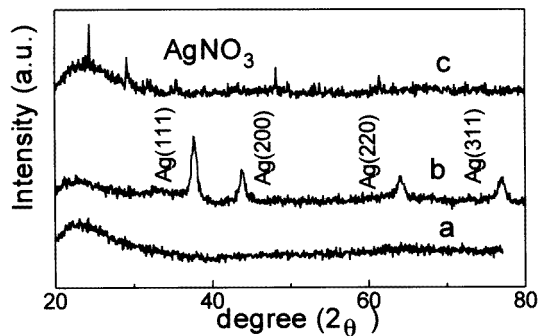


**Figure 1.** The x-ray diffractogram for: a, porous silica; b, soaked porous silica dried at up to 150 °C and c, sample b followed by heat treatment at 350 °C for 2 h.

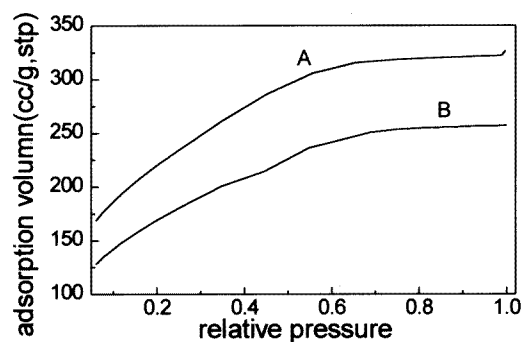


**Figure 2.** Nitrogen sorption isotherms of undoped sample (curve A, reference) and doped sample (curve B) after annealing at 350 °C for 2 h.

The monolithic porous silica was prepared with tetraethyl orthosilicate (TEOS), alcohol and water by the sol-gel technique, sufficiently cleaned with distilled water, dried and finally heat-treated at 600 °C for 2 h. The final porosity is estimated to be 50% by the pycnometry technique. The preformed monolithic porous silica was then soaked in a 0.25 M  $\text{AgNO}_3$  solution at room temperature (25 °C). After sufficient soaking (20 d or more), the sample was taken out and dried at a temperature from room temperature up to 180 °C to remove the solvent from it.  $\text{AgNO}_3$  crystallites certainly exist in the pores of the dried soaked sample. The x-ray diffractogram confirmed the presence of the  $\text{AgNO}_3$  crystallites, as curve b shows in figure 1. Then the dried sample was heated in air to 350 °C, and held for 2 h to let the  $\text{AgNO}_3$  decompose and leave only the silver particles in the silica, which has been shown by x-ray diffraction (see curve c in figure 1). The undoped sample was also subjected to the same treatment for reference.

The densities of the samples studied are obtained by the pycnometry technique. The amount of doped silver is estimated to be about 10 wt% by the density data of the doped and undoped samples. BET measurements using  $\text{N}_2$  gas (model ASAP 2000, made by Micromeritics) have indicated that the specific surface area decreases significantly from 760  $\text{m}^2 \text{g}^{-1}$  for the undoped sample to 460  $\text{m}^2 \text{g}^{-1}$  for the doped sample. This is attributed to the presence of Ag particles within the pores of the porous silica. This is more clearly

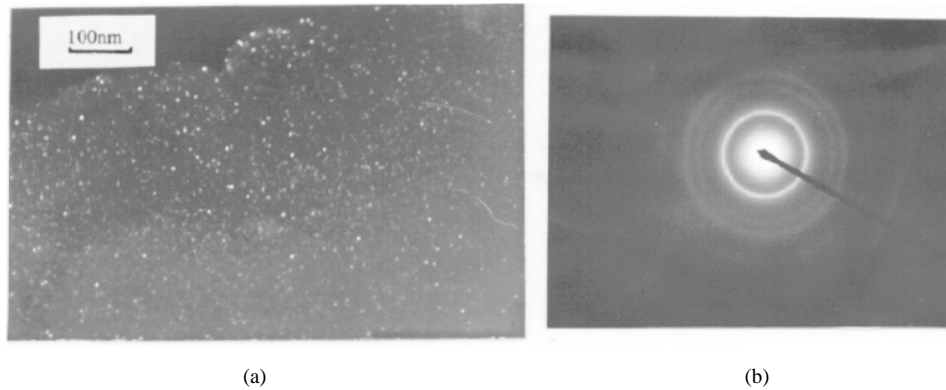


**Figure 3.** (a) An electron micrograph of the soaked sample dried at up to 150 °C and heat treated at 350 °C for 2 h; (b) the electron diffraction pattern of (a).

shown by the nitrogen sorption isotherms for the two samples (see figure 2). The whole curve for the doped sample is obviously lower than that for the reference sample. The slopes for the former are smaller than those of the latter in relative pressure less than 0.7, which corresponds to pores with diameter of less than 10 nm [12]. This means the doped Ag particles exist within pores of less than 10 nm in diameter.

The heat treated monolithic doped sample was ground. The powders so obtained were dispersed in acetone in a test tube. The latter was placed in an ultrasonic bath for 10 min. The clear liquid from the top portion of the test tube was taken and a few drops of the same were placed on a carbon coated copper grid. After evaporation of the acetone the copper grid was mounted on a JEM 200 CX transmission electron microscope operated at 200 kV, and hence the microstructure and selected area electron diffraction pattern were investigated: the size and distribution of microcrystals were inspected. Figure 3(a) is an electron micrograph for the doped sample; the particles are highly uniformly dispersed. Figure 3(b) is the selected area electron diffraction pattern from the micrograph shown in (a). The values of interplanar spacings have been calculated from the diameters of these rings in figure 3(b) and are given in table 1. The standard ASTM  $d_{hkl}$  values for silver are also shown in this table. The observed data indicate that the lattice parameter in the nano-sized silver particles is slightly larger than that in bulk silver, which is agreement with the x-ray diffraction results (as shown in table 1) obtained by comparing the bulk silver diffraction at the same diffractometer. The difference is of the order of 0.5–0.2%. This is probably associated with the small size of the particles, no compressive stress to the particles from the pore wall or the boundary coupling between Ag/SiO<sub>2</sub>, which will be further investigated. This result is opposite to those of the metal particles (including silver) with cubic structure and nanometer dimensions precipitated within a glass matrix [9]. In the latter, the lattice parameters for the metal nano-particles are slightly smaller than those of the corresponding bulk metals.

The histogram of the silver particle size was measured, as shown in figure 4. It can be well fitted with the log-normal distribution function given by

$$\Delta n = \frac{1}{\sqrt{2\pi} \ln \sigma} \exp \left\{ -\frac{1}{2} \left[ \frac{\ln(d/\bar{d})}{\ln \sigma} \right]^2 \right\} \Delta(\ln d)$$

where  $\Delta n$  is the fractional number of particles per logarithmic diameter interval  $\Delta(\ln d)$ ,  $\bar{d}$  is the average diameter and  $\sigma$  the geometric standard deviation. The average particle

**Table 1.** A comparison of  $d_{hkl}$  values (in nanometres) with ASTM data for silver nano-particles doped in porous silica.

Observed		
TEM	XRD	Standard silver
0.2398	0.2381	0.2359
0.2085	0.2068	0.2043
0.1468	0.1454	0.1445
0.1249	0.1236	0.1231
0.0943	—	0.0938

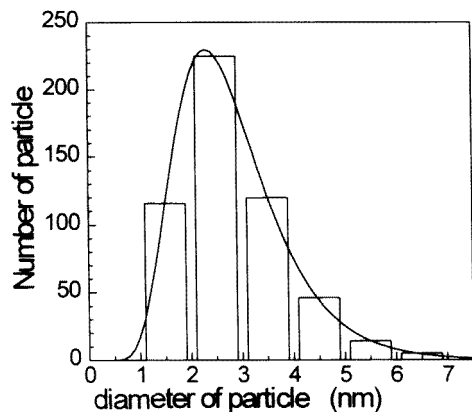


**Figure 4.** A histogram of the silver particle sizes in the doped porous silica shown in figure 3(a). The curve is the corresponding fitting result by the log-normal distribution function.

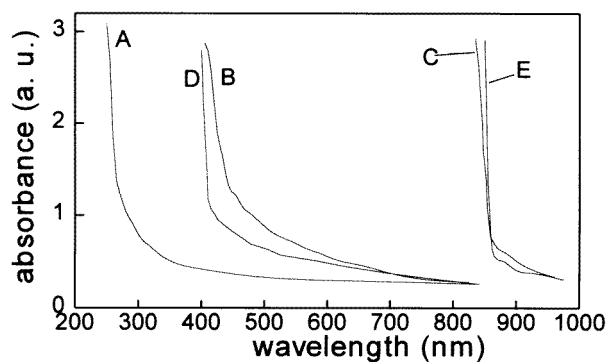


**Figure 5.** Optical absorption spectra for undoped and doped samples with different treatment conditions. A, undoped sample; B, doped sample after treating at 350 °C for 2 h; C, additional holding for 12 h in ambient air with relative humidity above 60% (25 °C) for sample B; D, additional treatment at 310 °C for 10 min in air for sample C; E, Ag<sub>2</sub>O powders of 20 nm diameter.

diameter for the doped sample is about 3 nm and  $\sigma$  is about 1.2 nm.

The optical absorption spectra for the doped and undoped monolithic samples with

a thickness of 0.5 mm were measured on a Cary 5E UV-VisNir spectrophotometer over the wavelength range 200–1000 nm. Figure 5 shows the optical absorption spectra for the reference and doped samples which were annealed followed by undergoing different procedures. Compared with the undoped sample (reference), there exists a large red-shift (>150 nm) of the absorption edge for the doped sample (see curves A and B in figure 5), but it is still transparent in the visible wave band (light yellow in colour). Further, we found that exposure to the ambient air at room temperature (25 °C) for the doped sample before optical measurement resulted in a transition from transparency to opacity, especially when exposed to air with high relative humidity. Curve C in figure 5 is the absorption spectrum for the doped sample exposed to the ambient air with relative humidity above 60% at 25 °C for more than 10 h after original heat treatment at 350 °C. The absorption edge shifts to 860 nm. At this time the sample becomes opaque (or black) in the whole visible band. No shift occurs after the doped sample is soaked in distilled water even for 10 d (at 25 °C). However, when the soaking is followed by drying at temperatures from 40 °C up to 150 °C, the absorption edge is also close to 900 nm; the curve is similar to curve C in figure 5 (not shown here). In addition, for the doped sample, after original annealing, exposure to dry air (relative humidity less than 10%) or lower temperature (< 10 °C) for a long time (a few weeks) results in an insignificant change in the absorption spectrum. Our results show that the response time for the transition from transparency to opacity depends on the exposure temperature, relative humidity and sample thickness. A thin sample, higher temperature (compared with room temperature) and high relative humidity in the ambient air cause a fast transition from transparency to opacity in the visible band.

The more interesting event is that this transition from transparency to opacity is reversible after the black sample is treated above 300 °C. When the sample corresponding to curve C in figure 5 was treated at 310 °C for 10 min, a transition from opacity to transparency occurred; the corresponding absorption spectrum is seen in curve D in figure 5. If this sample is exposed to ambient air with high relative humidity again, the transition from transparency to opacity soon reoccurs. This transition is reversible. Therefore, this new material assumes a memory effect, or optical switching phenomenon, in the process of alternating exposure to ambient air and annealing.

Now we briefly discuss the novel optical phenomenon of the reversible transition between transparency and opacity for the porous silica dispersed with silver nano-particles within its pores. This phenomenon is probably associated with the surface oxidation of the silver nano-particle, located within the pores of the porous silica, at moderate temperature with high relative humidity. The silver particles within the pores are open to the ambient air and in contact with oxygen in the air. In addition, they are small in size and chemically active [10]. The silver particles in contact with oxygen will undergo the reaction [13]  $\text{Ag} + \text{O}_2 \rightarrow \text{Ag}^+ + \text{O}_2^-_{\text{ads}}$  (ads, adsorption), or chemisorption occurs on the surface of the particles, followed by surface oxidation [14] (especially in air with high relative humidity). Silver oxide ( $\text{Ag}_2\text{O}$ ) is opaque in the visible band. Curve E in figure 5 is the spectrum of  $\text{Ag}_2\text{O}$  powder with diameter 20 nm. The absorption edge agrees with curve C in figure 5. However, the surface  $\text{Ag}_2\text{O}$  is unstable and will decompose when the temperature is above 300 °C [15]. Therefore, in the process of alternating exposure to the ambient air and annealing, the formation and decomposition of  $\text{Ag}_2\text{O}$  will alternately occur on the surface layer of the Ag particles within the pores of silica and hence result in the reversible transition between transparency and opacity, which has been confirmed by further experiments and will be reported in detail elsewhere.

In conclusion, we have presented a simple method for putting nano-sized silver particles into the pores of porous silica. The silver particles are highly uniformly dispersed within

pores of less than 10 nm in diameter in silica, and their size distribution can be fitted by a log-normal function. What is important is that in the process of alternating exposure to the ambient air and annealing this new material displays optical switching and a memory effect or reversible transition between transparency and opacity in the visible band, which is probably attributable to the alternating formation and decomposition of Ag<sub>2</sub>O on the surface layer of the doped Ag particles within the pores of the porous silica in different ambient conditions.

## References

- [1] Kuczynski J and Thomas J K 1985 *J. Phys. Chem.* **89** 2720
- [2] Coffey J L, Beauchamp G and Zerda T W 1992 *J. Non-Cryst. Solids* **142** 208
- [3] Tanahashi I and Mitsuyu T 1995 *J. Non-Cryst. Solids* **181** 77
- [4] Wu Chun-Guey and Thomas B 1994 *Science* **264** 1758
- [5] Rao S, Karaguleff C, Gabel A, Fortenbery R, Seaton C and Stegeman G 1985 *Appl. Phys. Lett.* **46** 801
- [6] Mennig M, Schmitt M, Kutsch B and Schmidt H 1995 *SPIE Proc.* **2288** 120
- [7] Judeinstein P and Schmidt H 1994 *J. Sol-Gel Sci. Technol.* **3** 189
- [8] Kundu K and Chakravorty D 1995 *Appl. Phys. Lett.* **66** 3576
- [9] Chatterjee A and Chakravorty D 1990 *J. Phys. D: Appl. Phys.* **23** 1097
- [10] Suryanarayana C 1995 *Int. Mater. Rev.* **40** 41
- [11] Komiyama H, Hayashi A and Inoue H 1985 *Japan. J. Appl. Phys.* **24** L269
- [12] At a given relative pressure  $x$ , the critical radius of the pore  $r = r_K + t$ , where  $r_K$  is the Kelvin radius (Thomson W 1871 *Phil. Mag.* **42** 448) and  $t$  the thickness of the sorption layer on the pore wall. In nitrogen sorption,  $r_K = -4.14(\log_{10} x)^{-1}$ ,  $t = -5.57(\log_{10} x)^{-1/3}$  (in units of Å) (Wheeler A 1955 *Catalysis* **2** 116). When  $x = 0.7$ ,  $r = 4$  nm and the pore diameter is less than 10 nm.
- [13] Kilty P A and Sachtler W M 1974 *Catal. Rev.* **10** 1
- [14] Brandes E A 1983 *Smithells Metals Reference Book* 6th edn (Boston, MA: Butterworth) pp 8–25
- [15] Weast R C 1989–1990 *CRC Handbook of Chemistry and Physics* 70th edn (Boca Raton, FL: Chemical Rubber Company) p B128